

An Overview of Wellhead Burning: Fundamental Science to Burn Performance Prediction

May 11-14, 2020

Steven G. Tuttle¹, Brian T. Fisher¹, David A. Kessler², Christopher J. Pfützner¹,
Aaron W. Skiba³, Rohit J. Jacob⁴

¹ Navy Technology Center for Safety and Survivability

² Laboratories for Computational Physics and Fluid Dynamics

³ American Society for Engineering Education (ASEE) Postdoctoral Associate

⁴ National Research Council (NRC) Postdoctoral Associate

Naval Research Laboratory
4555 Overlook Avenue, SW
Washington, DC 20375, USA
steven.tuttle@nrl.navy.mil

ABSTRACT

While wellhead burning has been an oil field hazard for generations, the development of capping response technologies and practices by industry experts has enabled the oil exploration community to shift its views of wellhead burning from a hazard to an oil spill response tool. This review covers some of the fundamental scientific aspects and technical issues of wellhead burning that engineers and policy makers will need to consider as this mitigation strategy is examined as a standard oil spill response tactic. For context, we examine a potential wellhead blowout scenario over a range of oil flows and examine the regimes of two-phase pipe flows, their dependence on wellbore velocities and gas-liquid ratios, and how those regimes will influence the burn efficiency with some insight from our experimental observations from two-phase spray burn testing. Among the critical findings that we present is that the worst-case discharge flow rate cannot be assumed to be the worst-case wellhead burning scenario.

INTRODUCTION

Wellhead fires have been an industry concern for many years for their danger, expense, and, at times, their necessity. They produce very large and visible burning plumes that require significant skill and expertise to extinguish. Though these fires are not trivial to extinguish, there are a number of companies that have developed the expertise to do so reliably and safely (Amer 2017, Garner 2017). With the maturation of these fire suppression techniques, wellhead fires can be viewed as a tool to manage and contain the environmental impact of wellhead spills if there are

favorable flow rates and properties of the gas and liquid. If favorable, wellhead burning can dispose more rapidly and inexpensively of wellhead effluent than should it fall on the ground or waterways; in such cases, more expensive dispersive and mechanical recovery tactics are the only remediation options.

One of the deadliest and most publicized surface wellhead blowouts occurred in 1982 at the Lodgepole sour gas well, located 130 km from Edmonton, Alberta, Canada (Zdeb 1982). This well created a plume of hydrogen sulfide (H_2S) that later ignited. After 68 days, 2 deaths, 16 injured, and millions of dollars of destruction, Boots and Coots extinguished the fire and capped the well. One of the eventual results were provincial regulations dictating the use of intentional wellhead ignition to manage the poisonous, flammable gas from sour wells, as specified by the ERCB Directive 14.3.6 (2017).

S.L. Ross/Energetex Study

One of the earliest analytical studies of wellhead blowout ignition and burning was performed by S.L. Ross Environmental Research and Energetex Engineering to provide decision making protocols for the Canada Oil and Gas Lands Administration in an effort to minimize environmental damage and human hazard (Ross 1986). Their 1986 report provides a broad primer, covering many of the fundamental details of wellhead blowout phenomena and the related engineering and environmental considerations of both subsea and surface blowouts. Without ignition and combustion, the well gas and evaporating condensate will drift with wind and mix with atmospheric oxygen to create a potentially hazardous explosive and/or poisonous zone. Thus, wellhead ignition provides a method to manage flammable and sour gas effluents while creating a dangerous fire.

In the same study, surface blowout crude oil and water effluents, their fallout behavior, and combustion efficiency were modeled for a range of gas-oil volume ratios (m^3/m^3), oil flow rates (m^3/day), and pipe diameters (Ross 1986). Though the authors never explicitly defined burn efficiency, they implied that the burn efficiency is the fraction of liquid crude oil or condensate that burns, evaporates, or drifts away in the wind (instead of falling back onto the ground) of the total ejected liquid. They recommended that predicted burn efficiency, cost, insurance

implications, and other factors be considered when deciding to ignite a wellhead. They suggest that if the predicted burn efficiency is less than 75%, intentional ignition should not be considered. Though this effort represents a significant addition to the body of literature, the investigators did not compare their predictions against data because none were available at that time.

Gulf War Aftermath

Wellhead blowout fires garnered significant public exposure after Iraqi military sabotaged over 700 Kuwaiti wellheads before fleeing U.S. Coalition forces and retreating back to Iraq during February 1991, near the end of the Gulf War, to create an unprecedented environmental disaster (EPA 1992, HSE 1992a, HSE 1992b). The burning wells not only blackened the air with soot, but also the desert with fallout of unburned crude oil. A number of reports were prepared by government agencies, contractors, and private entities to document the environmental and industrial damage.

An industry consortium was also assembled to investigate the large-scale hydrocarbon fire behavior and impact, effective response practices, extract understanding, and then document their findings to expand capabilities in response to such fires (HSE 1992a, HSE 1992b). From the report and photographs, it was clear that each wellhead fire was unique. Some formed a high, flaming plume with, or without, black, sooty smoke drifting from their tip. Other burning wellheads formed plumes that were encased in sooty smoke, a mist of falling residual oil, and produced slicks of unburned oil falling downwind. There were also wellheads that were surrounded by mounds of unburned coke fallout. Other wellheads expelled mixtures of oil and water that created white steam as the oil burned.

There was also a significant response from the scientific and engineering research communities to the Kuwaiti oil fires. A number of researchers traveled to the region to collect data from the emissions (Cahill *et al.* 1992, Cofer *et al.* 1992, Evans *et al.* 1991, Ferek *et al.* 1992, Hobbs and Radke 1992, Laursen *et al.* 1992), unburned crude oil fallout (Henry and Overton 1993, Kruge *et al.* 2018), and the combustion behavior of the wellhead fires (Evans *et al.* 1994, Herring and Hobbs 1994, Wade *et al.* 1995). Experimental and numerical studies were conducted to replicate the burn behavior of the wellhead fires to examine and elucidate their basic behavior and characteristics in

an effort to predict how two-phase fuel fires behave (Dutta *et al.* 1994a, Dutta *et al.* 1994b, Evans *et al.* 1994, Pfenning 1985, Wade *et al.* 1995). Absent from these studies were measurements of the spray droplet diameter distributions.

A careful examination of the Kuwaiti oil well fires and the wide range of reservoir and wellhead conditions suggest an infinitude of wellhead and reservoir conditions that can result in a blowout that does not have favorable burn behavior (EPA 1992, HSE 1992a, HSE 1992b). The wellhead pressure, gas-oil ratio (GOR), water content, surface damage and obstructions, and reservoir behavior all influenced how each wellhead burned. As a result, some wellheads burned the crude oil and condensates completely, while others deposited mounds of coke and pools of crude onto the Kuwaiti desert floor. For the Kuwaiti oil fires, those scenarios included wells with low GORs, high water fractions, and relatively low reservoir pressures, which are characteristic of reservoirs that have been significantly drained over time before there is a wellhead failure, such as the Timbalier failure (Flak *et al.* 1995) in the Gulf of Mexico. Other possible issues are obstructions that slow the flow of both gas and oil and narrow wellhead exits that create burn stability problems (McCaffrey and Evans 1988).

Recent Work

In November 2017, the Ocean Energy Safety Institute (OESI) hosted a peer review workshop entitled “Well Ignition as a Blowout Response” that provided a venue for industry, academic, and government to present their work on this topic. Siddhamshetty *et al.* (2019) then developed much of the presented work into an article. They expanded the methods first suggested by the S.L. Ross and Energetex (Ross 1986), used updated correlations, and accounted reservoir gas properties more carefully. The process they outlined to calculate the wellhead burn efficiency was as follows:

1. Determine the two-phase flow regime (bubbly, slug, churn, annular).
2. If annular, then determine the oil droplet size distribution.
3. Perform calculation determining the droplet evaporation and burning time scales to determine the flame height necessary to evaporate the droplets.
4. Perform a 0-dimensional heat release analysis from the gas to determine if sufficient heat is available to evaporate the liquid fuel.

5. Calculate the adiabatic flame temperature of the gas-phase flame and correct with radiant energy loss due to soot formation.
6. Quantify the radiant energy loss due to soot formation.

Sidhamshetty *et al.* then applied their approach to a worst-case discharge (WCD) case posited by Hilcorp for a potential well to predict an efficiency of 100% (Fitzgerald and Garner 2014, Hilcorp 2015, Hilcorp 2017). A careful examination of the process outlined above and of (Ross 1986, Siddhamshetty *et al.* 2019) will reinforce that they approached their calculations conservatively, but there are some caveats that the critical reader should consider.

Referring to Step 1, Siddhamshetty *et al.* (2019) did not elaborate on the ramifications of how the wider range of two-phase flow regimes (bubble, slug, and churn) would impact the effluent plume. In fact, their focus was on the wellbore flow, a topic on which they are experts, but they did not fully discuss how the wellbore flow would influence the ejected plume behavior, which directly influences the how much of the oil and gas burns and how much will either fall back to the surface or remain vapor. There was also a gap in the discussion over the annular flow entrainment fraction: the fraction of the liquid volume that has been entrained as droplets in the gas flow within the wellbore. A reader might incorrectly assume that annular flow in the wellbore would produce the same spray plume as that of a fully entrained mist, regardless of the entrainment fraction (Berna *et al.* 2014, Kataoka *et al.* 2000).

Referring to Step 2, we should note that the Liberty well conditions that Siddhamshetty *et al.* (2019) referenced were at significantly greater Re_G and Re_L than the validated range of the entrainment and droplet correlations (Berna *et al.* 2014, Berna *et al.* 2015a, Berna *et al.* 2015b, Kataoka *et al.* 1983, Kataoka *et al.* 2000). This does not invalidate their conclusions because a careful reading of these background papers reveal that as the gas flow rates increase, the general trend is for the entrainment to approach 100% and droplet diameters to decrease. However, the reader should note that conditions outside of the validated range of a correlation do not allow it to be used for reliable prediction of droplet diameters. We should also consider that the cited correlations only consider the entrained droplets and not those formed as the un-entrained annular liquid film is expelled and atomized, which can form a significant fraction of the oil volume.

Step 3 assumes the primary mechanism that drives poor burn efficiency is that the droplet lifetime (Shearer *et al.* 1979) is greater than the residence time within the burning plume. Though this is a potential a mechanism, it is not the only plausible mechanism. If we consider that much of the spray produced by flows with less than complete entrainment will be from the annular film and that the spray density of both the core and the periphery of the plume can be very high, two additional mechanisms are possible. One is that the larger droplets from the annular film are too large to evaporate or for the plume momentum to entrain them, so they fall to the ground. A related evaporation failure mechanism is that the droplet loading or number density is too great for all individual droplets to experience the same heat transfer and evaporation rate. This third failure mechanism is frequently neglected because traditional droplet evaporation or combustion analysis considers only a single droplet instead of a droplet ensemble or cloud that has as droplet density great enough to cool the gases surrounding the droplets. For now, each mechanism awaits thorough experimental validation.

There is a final, but more important, problem with the approach adopted by Siddhamshetty *et al.* (2019) that engineers, policy makers, and policy enforcers should note: there is an assumption that the WCD will produce the worst-case spill scenario. Our discussion below shows that these two scenarios should be considered distinct. The referenced correlations show that for a constant GOR, if the total flow rate decreases, then entrainment fraction will also decrease, the annular liquid film thickness will increase, and the peripheral droplet diameters will increase to much larger diameters than those at the core of the flow. The residence time of the larger droplets within the plume cannot be assumed to be long enough to evaporate and burn, whether they remain entrained in the plume or not (Berna *et al.* 2014, Fisher *et al.* 2018, Fisher *et al.* 2019, Kataoka *et al.* 2000). This work will explore wellhead blowout conditions and the associated spray physics and chemistry that inhibit the complete combustion of the liquid effluents.

RESERVOIR AND WELLHEAD CONSIDERATIONS

Before we explore the phenomena associated with wellhead blowout combustion, it is essential that we define the flow rate range that we will use for analysis and predictions. On the high end of

the flow rates, we will consider the WCD conditions used by Hasan and Kwon (2018) and Sidhamshetty et al. (2019) in consideration of the Liberty Project (Fitzgerald and Garner 2014, Hilcorp 2015, Hilcorp 2017, Rastegar 2017). The associated WCD flow rates and GOR are listed in Table 1.

Table 1 The predicted well and flow conditions for WCD of the Liberty Project (Fitzgerald and Garner 2014, Hilcorp 2015, Hilcorp 2017). Values are in SI and in industry-standard units. Oil properties are from Hilcorp (2017), which were in comparison to Endicott properties (AOGCC 2018, ECCO 2001).

Parameter	Crude Oil	Reservoir Gas
Worst-case Discharge		
Flow		
(m ³ /s)	0.168	26.1
(BBL/day)	91,200	
(SCF/day)		7.95×10 ⁷
GOR		
(m ³ /m ³)		155
(SCF/BBL)		872
Exit Temp.		
(K)		366
(°F)		199
API (°)	24-27	-
Density (kg/m³)	900	0.663
Viscosity (Pa*s@298 K)	0.0762	
(Pa*s@366 K)	0.0254	1.33×10 ⁻⁵
Surface Tension (N/m)	0.019	-
Pipe Diameter (mm)		216
Superficial Reynolds Number	3.5×10 ⁴	7.7×10 ⁶

The maximum, or WCD, Liberty flow conditions provide the quantitative ceiling to our study and provide insight into the orders of magnitude of the flows we need to consider. Such potentially high oil and gas flow rates are typical for some new wells, though the maximum gas or oil flow rate will vary significantly between wells and reservoirs. Once a reservoir starts producing gas and oil, the reservoir pressure decreases and the maximum potential flow rates also decrease, even with gas injection. Therefore, our solution space needs to consider that either the gas or the oil flow rate may be any value between zero to values similar to those in Table 1, depending on the well depth, reservoir, and other engineering details.

The thermophysical properties of the oil and gas depends upon the temperature and the reservoir, which can vary widely. Most oil assays report properties at 298 K, while the estimated Liberty wellhead temperature is 366 K. Since our objective is to not represent a single case but the broader solution space, we will make some assumptions and estimations. We will assume that the

viscosity is roughly that of Endicott's reservoir conditions of 1.09 cP (AOGCC 2018), and that the surface tension is equal to n-decane at the same temperature, 0.019 N/m (Lemmon *et al.* 2019). For gas properties, we will assume those of methane, since the bulk of the gas from reservoirs with both oil and gas is methane (Lemmon *et al.* 2019). These will provide order-of-magnitude ranges from which we can calculate predictions and draw conclusions.

REVIEW OF WELLHEAD BEHAVIOR

There are a number of relevant physical and chemical behaviors that should be covered, but due to the constraints of space, we will restrict our discussion to a limited number of topics. Additional topics will be included in a full-length journal review.

Wellbore Flow

One of the most important questions we need to consider for a wellhead blow out is how the two-phase wellbore flow will influence the wellhead ejection behavior and the resulting two-phase flow structure of the spray plume. The liquid and gas dynamics of the pipe, wellhead, and plume flows are a result of the change in phase between the reservoir and the wellhead, the resulting high-speed pipe and flows, and the expansion of the plume.

In the process, these flows can exhibit specific patterns, depending on the liquid-to-gas ratio, pipe angle, and fluid properties. Understanding and predicting these behaviors is an ongoing research topic that is relevant to a wide range of chemical transportation and processing applications (Berna *et al.* 2014, Hasan and Kabir 2018a, Lips and Meyer 2011, Rouhani and Sohal 1983, Taitel *et al.* 1980). For this paper, we will constrain our discussion to vertical pipes.

It is instructive to go back to the model of the fluid rising up from a reservoir to understand these patterns. In the reservoir, the gas is frequently at supercritical pressures and temperatures so that the gas and crude oil are in solution. As they flow up through the riser or wellbore, the decreasing pressure allows the gases to evaporate and separate. Initially, small bubbles will form in the flow (bubbly flow). As the bubbles increase in size, they agglomerate such that the flow forms axially distinct regions of gas and liquid in the flow (slug flow). As the gas fraction increases, the distinct sections begin to mix and collapse upon one another to form churn flow.

Finally, as the gas fraction increases further, the gas volumetric flow rate is large enough to form a contiguous flow at the center of the flow. The remaining liquid initially forms an annulus at the wellbore wall that is sheared by the gas flow to form droplets that deposit and are sheared again in steady, dynamic equilibrium (annular flow). With sufficient gas flow rate and/or volume fraction increase, the film is thin enough to be negligible (mist or dispersed regime). Since the distance between the reservoir and the wellhead is so long, it is reasonable to assume that the flow behavior is in equilibrium and fully developed at any one point, including at the wellhead, upstream of the exit plane.

The difficulty in predicting these transitions is discussed in the textbook by Hasan and Kabir (2018b). They noted that each regime shift is accompanied by a shift in the fluid mechanic behavior and highlighted the considerable influence wellbore pressure has on the separation of the gas and liquid.

We can assume that for an annular flow, the ejected flow will form some sort of spray structure, but it is unclear what kind of flow structures form when bubbly, slug, or churn flows are ejected through a wellhead. It is reasonable to assume that these lower velocity flows are more likely to form pools or fountains; neither of which burn efficiently. Therefore, for the sake of brevity and simplicity, we will focus on the annular and mist flow regimes.

The characteristics of the annular flow that will influence the plume are the film thickness, liquid entrainment fraction, and the droplet formation. The annular film thickness will directly influence the droplet diameter distribution of the annular spray region, as shown by Fisher et al. (2018, 2019), while the liquid entrainment fraction will directly influence how much liquid ends up in that annular spray region or as fine droplets in the central core of the flow. Finally, the wellbore-entrained droplets will form the spray at the center of the plume.

The interaction between the liquid annular film and the gas flowing through the center, as discussed in the reviews by Berna *et al.* (2014, 2015b), drives the formation of instability surface waves on the liquid film, the formation and stretching of ligaments, which then break apart to form droplets. The higher velocity gas convects the droplets axially, while the three-dimensional, unsteady turbulence convects them transversely until they eventually collide back against the

wellbore wall.

The liquid film thickness, δ , denotes the average thickness with the presence of surface waves and other perturbations. This metric has been overlooked wellhead blowout discussions, even though the film can drive the formation of much larger droplets upon ejection than the entrained droplets at the center of the flow (Fisher *et al.* 2018, Fisher *et al.* 2019). A review of droplet entrainment behaviors by Berna *et al.* (2014) describes the two-phase flow regimes for horizontal and vertical pipes, liquid wave behavior and characteristic metrics, and the significant research in correlating these metrics to dimensionless flow numbers. Berna *et al.* (2014) developed a correlation with an R^2 fit of 90%, which if we use the range of Liberty conditions in Table 1 and calculate δ for a range of Re_L , we create the top plot shown in Figure 1.

For each curve, the gas flow rate ranges between 0.001 to 2.740 m^3/s and the corresponding oil flow rate for a fixed GOR, velocities, thermophysical properties, and dimensionless numbers were calculated and then plugged into the Berna *et al.* (2014) correlation for δ/D . The Liberty WCD range, though the GOR changes over time, corresponds to $3.02 \times 10^5 \leq Re_L \leq 8.18 \times 10^5$, which was highlighted green in the top plot and subsequent plots of Figure 1. The line patterns (dashed, continuous, and dash-dot-dash) denote GORs of 2000, 872, and 500 SCF/BBL (356, 155, and 51 m^3_{gas}/m^3_{oil}), respectively.

The δ plots of Figure 1, top, suggest a number of significant behaviors and implications that should be noted. First, there is the general, predictable trend that increasing the Re_L (for a fixed GOR) or the GOR (for a fixed Re_L) decreases the film thickness while decreasing the same increases the film thickness. Most importantly, the plots of film thickness show that for much of the range of Re_L , the film thickness is non-negligible, especially if correspondingly-scaled droplets form from that film upon ejection.

Recent entrainment correlations, referenced in Siddhamshetty *et al.* (2019) from both Kataoka *et al.* (2000) and Berna *et al.* (2015b), have been referenced in industry and government reports (Conroy *et al.* 2016). The correlations within these two papers provide a broad set of mathematical relations that describe entrainment, the axial distance required for quasi-equilibrium, and the distance required for full entrainment. Entrainment is defined as the fraction of the total liquid

mass that is entrained into the gas flow in the form of droplets. We will denote the quasi-equilibrium entrainment by E_∞ and calculate using the expressions from Kataoka *et al.* (2000) and Berna *et al.* (2015b).

The entrainment plot in Figure 1, middle, compares correlated predictions for the Kataoka and Berna correlations for a range of Re_L and three different values of GOR. The most significant aspect of the plot is that the 30-day period of the example Liberty WCD is 100% entrained. Increasing the GOR correspondingly increases the entrainment, while decreasing the GOR also decreases entrainment, as we might expect.

The entrained, volume mean droplet diameter correlations referenced in Siddhamshetty *et al.* (2019) were those developed by Kataoka *et al.* (1983) and a later correlation developed Berna *et al.* (2015b) that accounts for higher pressures. The D_{vm} plots in Figure 1, bottom, reveal a number of behaviors that should be considered in the context of wellhead flows. First, the Liberty worst-case discharge conditions, over the first 90 days of a free-flowing wellhead, are well outside of the validated range for both correlations, though the exact limits of data referenced by the Berna correlation is still being determined. Though we can expect that the trends are qualitatively accurate, we cannot use the droplet diameters predicted outside of the validated range of the correlations to make quantitative burn efficiency predictions. The extrapolated trend for the Liberty WCD conditions suggests that the droplet diameters are in the range between 10 and 100 μm . Though this is a wide range and unsubstantiated from the data cited by Kataoka *et al.* (1983) and Berna *et al.* (2015a), the correlations predict that the droplet diameters should generally decrease as We_G , Re_L , and Re_G increase, since the liquid-gas interface shear, which drives droplet formation, would correspondingly increase to form smaller droplets. Such trends are similar for the film thickness and entrainment fractions.

In comparing the δ , E_∞ , and D_{vm} plots, there are a number of behaviors we should consider. First, for decreasing values of Re_L without full entrainment, the annular film thickness is large enough that if it were to develop into comparatively-sized droplets, they may not evaporate and burn if they are convected to the outer edges of the gas-air shear layer and fall to the ground.

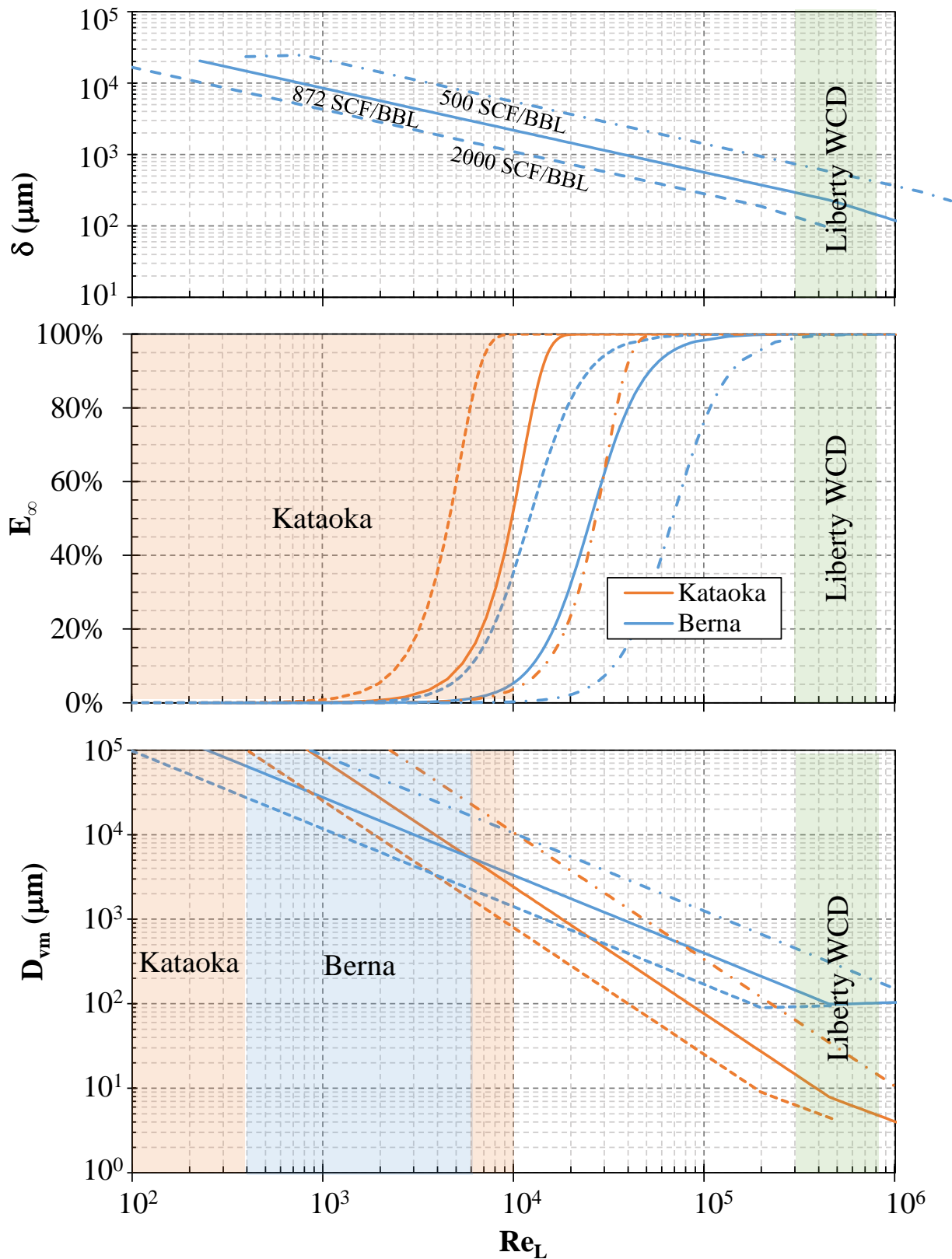


Figure 1 Plotted δ , E_∞ , and D_{vm} for a range of Re_L , with the first thirty days of Liberty WCD highlighted green. The validated range of the Kataoka *et al.* correlation shown highlighted orange and the validated range of Berna *et al.* is highlighted blue.

Second, even the fully entrained droplets are quite large for $Re_L \leq 10^4$, suggesting that as the flowrate of a wellhead decreases, the droplet formation behavior will not produce an efficiently burning plume.

Wellhead Ejection and Combustion

Figure 2 shows how the crude oil and well gas form a flame and diagrams the potential products that are formed. There are two potential fates of the oil: *oleum evanescet* and *oleum ruinam*. The disappeared oil, *oleum evanescet*, completely burns into gaseous products (CO_2 , CO , H_2O , SO_x , NO_x and unburned hydrocarbon (UHC) vapor) and soot that is carried away by the atmosphere. The residue and oil that falls upon the ground, *oleum ruinam*, is composed of soot

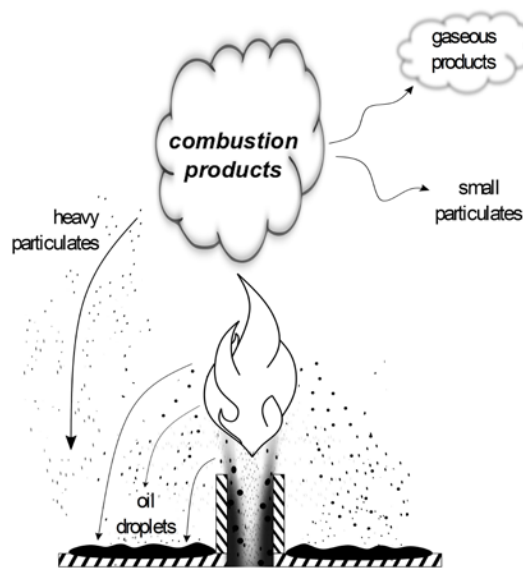


Figure 2 Diagram of wellhead spray combustion behavior and the fate of the two-phase fuels.

agglomerates and droplets ranging from those partially evaporated or burned to large droplets splattered close to the wellhead (EPA 1992, HSE 1992a, HSE 1992b). The wellbore behavior that determines the fate of the ejected crude oil depends on the GOR and the flow rates of the respective wellbore's two phase flow regime. For now, we will focus on the annular and mist flow patterns that will produce a combusting spray.

In such a flow, the entrained, dispersed droplets do not undergo any immediate changes unless there are shock structures present (Lin and Hermanson 2014), while the expelled annular film is sheared into ligaments, which then form droplets; a common process in almost all atomizing systems (Faeth 1999). Droplet formation from an annular film is of interest because of its applicability to air or gas-assisted atomization processes (Cohen and Rosfjord 1993, Lasheras and Hopfinger 2000, LeFebvre 1989, Senecal *et al.* 1999, Shanmugasadas and Chakravarthy 2017). Unfortunately, these studies employ much shorter development lengths than those of a wellbore. In response, we have developed an atomizer to examine these sprays in the laboratory, as described by Fisher *et al.* (2018, 2019), that mimics the wellbore atomization process. This open pipe atomizer (OPA) allows both the gas and liquid to develop to quasi-equilibrium because of its long

development length and allows the examination of droplet formation, transport, evaporation, and combustion. We would like to review the current state of research of the spray mechanics and the combustion behavior of the OPA.

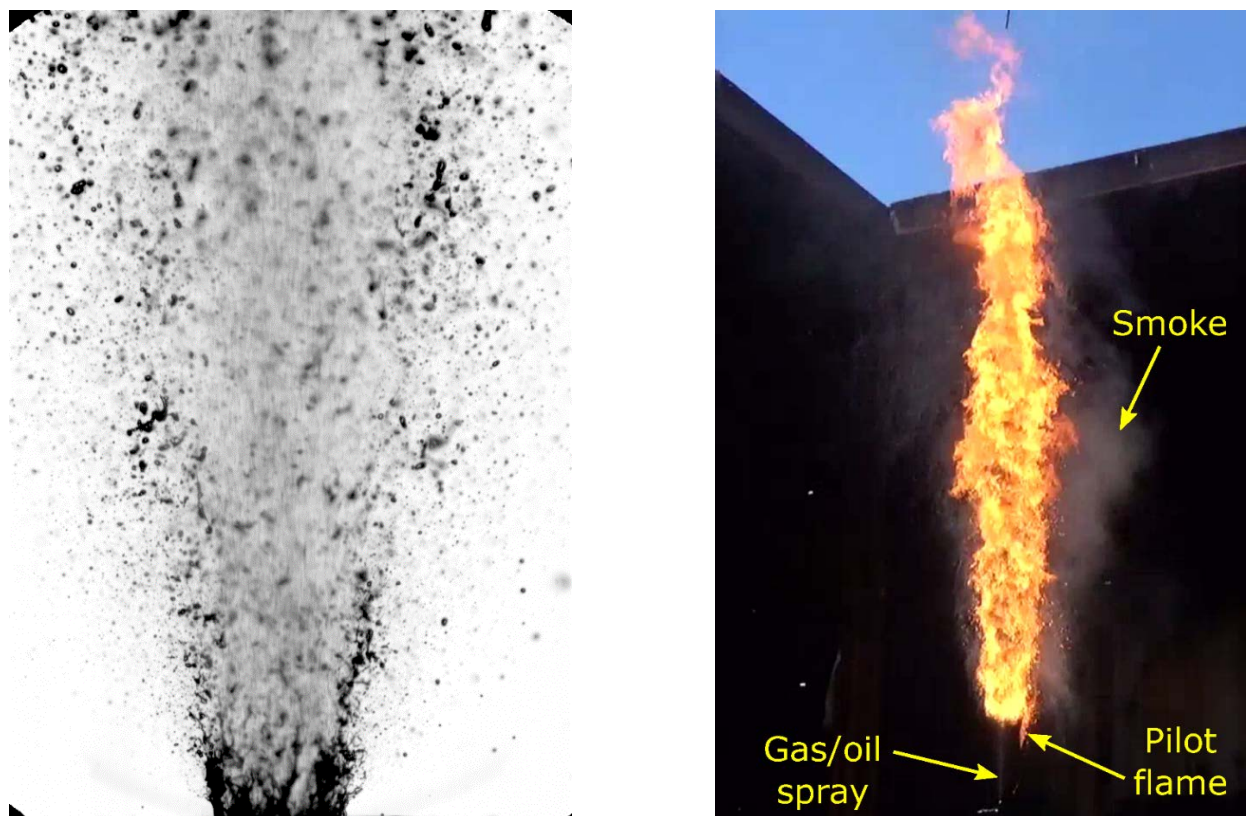


Figure 3 (L) Diffuse backscatter imaging of spray from annular flow out of a laboratory-scale ($D=0.84$ mm), OPA described by Fisher *et al.* (2018, 2019). The scale of the image is approximately 4.6 mm wide by 6.7 mm high. The flow rates are 0.4 g/s of air and 0.8 g/s of water, for a GOR of $228 \text{ m}^3_{\text{air}}/\text{m}^3_{\text{water}}$. **(R)** Still image from reduced-scale OPA ($D=8.5$ mm) flowing 3 g/s of 80% CH_4 -5% C_2H_6 -15% C_3H_8 and 16 g/s of Endicott crude oil, for a GOR of $135 \text{ m}^3_{\text{gas}}/\text{m}^3_{\text{oil}}$ (760 SCF/BBL).

Recent work reported by Fisher *et al.* (2018, 2019) examined aspects of annular flow-driven open pipe atomization. Both studies were based on laboratory flows using ethane and heptane as gaseous and liquid fuels, respectively. Using phase Doppler anemometry and high-speed diffuse back-scatter illumination (HS-DBI) (Westlye *et al.* 2017), they discovered that the spray plume from an annular flow produced two distinct spray regions: an inner core of high-speed, small droplets and an outer region of relatively slower, larger droplets formed by the shear of the annular film.

More recent, unpublished work by this group is examining the droplet formation process using

HS-DBI of the exit of the open pipe atomizer to examine the details of the annular film ejection and droplet formation process. Figure 3L shows a HS-DBI image of an OPA ($D=0.85$ mm) producing an annular, two-phase flow, as reported previously by Fisher *et al.* (2018, 2019). At the base and in the outer diameter of the plume, where the film is ejected from the OPA, there is a region of large ligament formation, stretching, and pinching to form droplets much larger than the entrained droplets at the center of the flow, which were formed upstream in the pipe. As discussed earlier, this non-uniformity persists downstream.

A larger-scale study by the same group currently underway is measuring burn efficiency from a reduced-scale OPA ($D = 8.4$ mm) ejecting synthetic reservoir gas (80% CH_4 -5% C_2H_6 -15% C_3H_8) and crude oil (Fisher *et al.* 2020), shown in Figure 3R. They discovered that at the conditions of their study, the bulk of the fallout was from the peripheral droplets that originated from the annular film. A careful examination of the photograph in Figure 3R shows burning droplets and smoke-trailing droplets in the process of falling out of the plume.

CONCLUSIONS

A careful analysis of past wellhead burning from Kuwait and the Gulf of Mexico highlight that wellhead failures and the resulting fires can assume a broad range of configurations, depending on the reservoir and wellhead conditions. An example WCD case was used as a starting point to examine how the flow regime can shift with a reduction of flow rate or changes in GOR, highlighting that the WCD of a well may not actually be the worst-case scenario for a spill. A wellbore or wellhead obstructions that slow flow rates well below the anticipated WCD rates can shift the flow regime from fully entrained mist, which will burn very efficiently, to a poorly entrained annular flow that produces large droplets and heavy fallout. This regime shift is simply due to the reduced flow rate, not to changes in GOR.

Recent experimental work from the author's group has suggested that there are additional mechanisms for poor wellhead burn efficiency. The previously assumed mechanism is that the droplet evaporation timescale is greater than the burn plume residence timescale. Experimental investigations have shown that droplets formed from the annular film are large enough to fall out

of the plume. An additional mechanism may be that the total droplet loading or density may be great enough to resist full evaporation within the plume.

ACKNOWLEDGEMENTS

This study was funded by the U.S. Department of the Interior, Bureau of Safety and Environmental Enforcement through Interagency Agreement E15PG00022 with the Naval Research Laboratory.

REFERENCES

ERCB DIRECTIVE 071 14.3.6, 2017. Emergency Preparedness and Response Requirements for the Petroleum Industry.

Amer, M. 2017. Well Ignition and Capping Experience. Well Ignition as a Blowout Response: A Peer Review Workshop for Dialogue. Ocean Energy Safety Institute, Houston, TX, 2017.

AOGCC, 2018. Reservoir Properties. Pool Statistics, Alaska Oil and Gas Conservation Commission, Anchorage, USA.

http://aogweb.state.ak.us/poolstatistics/annual/current/OIL/Endicott,Endicott_Oil/Reservoir_Properties.html (last accessed October 10, 2019).

Berna, C., Escrivá, A., Muñoz-Cobo, J. L., and Herranz, L. E. 2014. Review of droplet entrainment in annular flow: Interfacial waves and onset of entrainment. *Progress in Nuclear Energy* 74: pp. 14-43.

Berna, C., Escrivá, A., Muñoz-Cobo, J. L., and Herranz, L. E. 2015a. Development Of New Correlations For Annular Flow. *Computational Methods in Multiphase Flow VIII*. WIT Press, pp. 451-462.

Berna, C., Escrivá, A., Muñoz-Cobo, J. L., and Herranz, L. E. 2015b. Review of droplet entrainment in annular flow: Characterization of the entrained droplets. *Progress in Nuclear Energy* 79: pp. 64-86.

Cahill, T. A., Wilkinson, K., and Schnell, R. 1992. Composition analyses of size-resolved aerosol samples taken from aircraft downwind of Kuwait, spring 1991. *Journal of Geophysical Research: Atmospheres* 97:D13: pp. 14513-14520.

Cofer, W. R., Stevens, R. K., Winstead, E. L., Pinto, J. P., Sebacher, D. I., Abdulraheem, M. Y., Al-Sahafi, M., Mazurek, M. A., Rasmussen, R. A., Cahoon, D. R., and Levine, J. S. 1992. Kuwaiti oil fires: Compositions of source smoke. *Journal of Geophysical Research: Atmospheres* 97:D13: pp. 14521-14525.

Cohen, J. M., and Rosfjord, T. J. 1993. Influences on the Sprays Formed by High-Shear Fuel Nozzle/S wirlers Assemblies. *Journal of Propulsion and Power* 9:1: pp. 16-27.

Conroy, M. W., Ananth, R., and Tuttle, S. G. 16 February 2016. Preliminary Technical Guidance and Literature Review to Assist in Evaluation of Wellhead Burning as a Blowout Response. Bureau of Safety and Environmental Enforcement, OSRR-1063AA. Sterling, VA.

Dutta, P., Gore, J. P., Sivathanu, Y. R., and Sojka, P. E. 1994a. Global properties of high liquid loading turbulent crude oil + methane/air spray flames. *Combustion and Flame* 97:3-4: pp. 251-260.

Dutta, P., Sivathanu, Y. R., and Gore, J. P. June 1994. An Investigation of Oil and Gas Well Fires and Flares. National Institute of Standards and Technology, NIST-GCR-94-653. West Lafayette, Indiana.

ECCC, 2001. Oil Properties. ESTC, Environment and Climate Change Canada, Ottawa, Canada. http://www.etc-cte.ec.gc.ca/databases/OilProperties/oil_prop_e.html (last accessed October 10, 2019).

EPA. 1992. United States Gulf Environmental Technical Assistance. U.S. Environmental Protection Agency.

Evans, D. D., Madrzykowski, D., and Haynes, G. A. 1994. Flame Heights and Heat Release Rates of 1991 Kuwait Oil Field Fires. 4th International Symposium of International Association for Fire Safety Science. pp. 1279-1289 International Association for Fire Safety Science, Ottawa, Ontario, Canada, 1994.

Evans, D. D., Walton, W. D., Baum, H. R., Mulholland, G. W., Lawson, J. R., Koseki, H., and Ghoniem, A. F. 12-14 June 1991. Smoke Emission From Burning Crude Oil. National Institute of Standards and Testing, NIST SP 995. Vol. 2.

Faeth, G. M. 1999. Liquid Atomization in Multiphase Flows - A Review. AIAA 30th Fluid Dynamics Conference. American Institute of Aeronautics and Astronautics, Norfolk, VA, 1999.

Ferek, R. J., Hobbs, P. V., Herring, J. A., Laursen, K. K., Weiss, R. E., and Rasmussen, R. A. 1992. Chemical composition of emissions from the Kuwait oil fires. *Journal of Geophysical Research: Atmospheres* 97:D13: pp. 14483-14489.

Fisher, B. T., Kessler, D. A., Tuttle, S. G., and Tuesta, A. D. 2018. Experimental Measurements and Numerical Simulations of Droplet Behavior in a Heptane/Ethane Spray Flame. 41st AMOP Technical Seminar on Environmental Contamination and Response. pp. 985-1011 Environment and Climate Change Canada, Victoria, British Columbia, Canada, 2018.

Fisher, B. T., Tuttle, S. G., Jacob, R. J., Pfützner, C. J., Tuesta, A. D., and Kessler, D. A. 2019. High-Speed Imaging of Atomization Behavior and Temperature Field in Spray Flames that Simulate Oil Wellhead Fires. 42nd AMOP Technical Seminar on Environmental Contamination and Response. pp. 663-679 Environment and Climate Change Canada, Halifax, Nova Scotia, Canada, 2019.

Fisher, B. T., Tuttle, S. G., Pfützner, C. J., and Kessler, D. A. 2020. Experimental Approach for Measuring Burn Efficiency of a Reduced-Scale Wellhead Fire. IOSC. pp. XXX-YYY International Oil Spill Conference, New Orleans, LA, 2020.

Fitzgerald, S., and Garner, J. B. 29 December 2014. Hilcorp Liberty Project Burn Efficiency Evaluation: Final Report. Boots & Coats: A Halliburton Service, (Proprietary).

Flak, L. H., Kelly, M. J., and Tuppen, J., 1995. Case history of Timbalier blowout shows necessity of capping while burning. Offshore Magazine.
<https://www.offshore-mag.com/business-briefs/equipment-engineering/article/16762376/well-control-technology-case-history-of-timbalier-blowout-shows-necessity-of-capping-while-burning> (last accessed 29 April 2019).

Garner, J. 2017. Well Capping While Burning. Well Ignition as a Blowout Response: A Peer Review Workshop for Dialogue. Ocean Energy Safety Institute, Houston, TX, 2017.

Hasan, A. R., and Kabir, C. S. 2018a. Fluid Flow and Heat Transfer in Wellbores, 2nd ed., Society of Petroleum Engineers, Richardson, Texas, 2018a.

Hasan, A. R., and Kabir, C. S. 2018b. Multiphase Flow: Mechanistic Models for Vertical Walls. Fluid Flow and Heat Transfer in Wellbores. 2nd ed., Society of Petroleum Engineers, Richardson, Texas.

Hasan, A. R., and Kwon, J. 10 January 2018. Literature Review for Understanding of Well-Ignition as a Blowout Response: A White Paper. Ocean Energy Safety Institute. College Station, Texas.

Henry, C. B., and Overton, E. B. 1993. Chemical Composition and Source Fingerprinting of Depositional Oil from the Kuwaiti Oil Fires. International Oil Spill Conference Proceedings. 1993: pp. 407-413 American Petroleum Institute, Tampa, Florida, 1993.

Herring, J. A., and Hobbs, P. V. 1994. Radiatively driven dynamics of the plume from 1991 Kuwait oil fires. Journal of Geophysical Research: Atmospheres 99:D9: pp. 18809-18826.

Hilcorp. Liberty Development Project Development and Production Plan (Revised). Hilcorp Alaska, LLC. Vol. 2015.

Hilcorp. 2017. Liberty Overview. Well Ignition as a Blowout Response: A Peer Review Workshop for Dialogue. Ocean Energy Safety Institute, Houston, TX, 2017.

Hobbs, P. V., and Radke, L. F. 1992. Airborne Studies of the Smoke from the Kuwait Oil Fires. Science 256:5059: pp. 987-992.

HSE. July 1992. Kuwait Scientific Mission - Mission Overview. The Steel Construction Institute, OTH 94 450. Vol. 1, Berkshire.

HSE. July 1992. Kuwait Scientific Mission - Technical Report. The Steel Construction Institute. Vol. 2, Berkshire.

Kataoka, I., Ishii, M., and Mishima, K. 1983. Generation and Size Distribution of Droplet in Annular Two-Phase Flow. *Journal of Fluids Engineering* 105:2: pp. 230-238.

Kataoka, I., Ishii, M., and Nakayama, A. 2000. Entrainment and desposition rates of droplets in annular two-phase flow. *International Journal of Heat and Mass Transfer* 43:9: pp. 1573-1589.

Kruger, M. A., Gallego, J. L. R., Lara-Gonzalo, A., and Esquinas, N. 2018. Chapter 7 - Environmental Forensics Study of Crude Oil and Petroleum Product Spills in Coastal and Oilfield Settings: Combined Insights From Conventional GC-MS, Thermodesorption-GC-MS, and Pyrolysis-GC-MS. *Oil Spill Environmental Forensics Case Studies*. Butterworth-Heinemann, pp. 131-155.

Lasheras, J. C., and Hopfinger, E. J. 2000. Liquid Jet Instability and Atomization in a Coaxial Gas Stream. *Annual Review of Fluid Mechanics* 32:1: pp. 275-308.

Laursen, K. K., Ferek, R. J., Hobbs, P. V., and Rasmussen, R. A. 1992. Emission factors for particles, elemental carbon, and trace gases from the Kuwait oil fires. *Journal of Geophysical Research: Atmospheres* 97:D13: pp. 14491-14497.

LeFebvre, A. H. 1989. *Atomization and Sprays*, 1 ed., Hemisphere Publishing Corporation, 1989.

Lemmon, E. W., McLinden, M. O., and Friend, D. G. 2019. Thermophysical Properties of Fluid Systems. NIST Chemistry WebBook, NIST Standard Reference Database Number 69. National Institute of Standards and Technology, Gaithersburg MD, 20899.

Lin, E. P., and Hermanson, J. C. 2014. Compression Wave Structure on Droplets under Supersonic Conditions. 50th AIAA/ASME/SAE/ASEE Joint Propulsion Conference. American Institute of Aeronautics and Astronautics, 2014.

Lips, S., and Meyer, J. P. 2011. Two-phase flow in inclined tubes with specific reference to condensation: A review. *International Journal of Multiphase Flow* 37:8: pp. 845-859.

McCaffrey, B. J., and Evans, D. D. 1988. Very large methane jet diffusion flames. *Symposium (International) on Combustion* 21:1: pp. 25-31.

Pfenning, D. B. January. Final report for blowout fire simulation tests. National Bureau of Standards, NBS-GCR-85-484.

Rastegar, R. 2017. Liberty WCD Scenario. Well Ignition as a Blowout Response: A Peer Review Workshop for Dialogue. Ocean Energy Safety Institute, Houston, TX, 2017.

Ross, S. L. Decision-Making Aids for Igniting or Extinguishing Well Blowouts to Minimize Environmental Impacts. Environmental Studies Revolving Funds, Canada Oil and Gas Lands Administration. Waterloo, Ontario.

Rouhani, S. Z., and Sohal, M. S. 1983. Two-phase flow patterns: A review of research results. *Progress in Nuclear Energy* 11:3: pp. 219-259.

Senecal, P. K., Schmidt, D. P., Nouar, I., Rutland, C. J., Reitz, R. D., and Corradini, M. L. 1999. Modeling high-speed viscous liquid sheet atomization. *International Journal of Multiphase Flow* 25:6: pp. 1073-1097.

Shanmugadas, K. P., and Chakravarthy, S. R. 2017. A canonical geometry to study wall filming and atomization in pre-filming coaxial swirl injectors. *Proceedings of the Combustion Institute* 36:2: pp. 2467-2474.

Shearer, A. J., Tamura, H., and Faeth, G. M. 1979. Evaluation of a Locally Homogeneous Flow Model of Spray Evaporation. *Journal of Energy* 3:5: pp. 271-278.

Siddhamshetty, P., Ahammad, M., Hasan, R., and Kwon, J. 2019. Understanding wellhead ignition as a blowout response. *Fuel* 243: pp. 622-629.

Taitel, Y., Bornea, D., and Dukler, A. E. 1980. Modelling flow pattern transitions for steady upward gas-liquid flow in vertical tubes. *AIChE Journal* 26:3: pp. 345-354.

Wade, R., Sivathanu, Y. R., and Gore, J. P. October 1995. A Study of Two Phase High Liquid Loading Jet Fires. U.S. Department of Commerce, National Institute of Standards and Technology, NIS-GCR-95-678. Gaithersburg, MD.

Westlye, F. R., Penney, K., Ivarsson, A., Pickett, L. M., Manin, J., and Skeen, S. A. 2017. Diffuse back-illumination setup for high temporally resolved extinction imaging. *Applied Optics* 56:17: pp. 5028-5038.

Zdeb, C. 1982. Lodgepole sour gas well blowout finally capped. *Edmonton Journal*. Edmonton, Alberta, 1982.